CHAPTER VII
Synthesis of the Results and Conclusions

For this thesis detailed maps of the stellar structure and the H II kinematics were obtained for the five galaxies NGC 3810, NGC 3893, NGC 4254, NGC 5676 and NGC 6643. The observations were compared to the results from a set of hydrodynamic gas simulations. The simulations were performed for realistic two dimensional gravitational potentials, combined from stellar disk and dark halo contributions. The gravitational potential of the stellar disk was derived directly from the observations of the galaxies, using color-corrected NIR photometry to represent the stellar mass fraction. For the dark halo, the mass density distribution was chosen to be an axisymmetric isothermal sphere with a core. The potential of the halo was calculated in the two-dimensional plane of each galaxy's disk. The sequence of potentials was assembled by preselecting certain disk mass fractions and adjusting the halo parameters so that the rotation curve emerging from the total potential matches the mean observed H II rotation curve. The hydrodynamic simulations were performed by using the BGK hydro-code, contributed by Adrianne Slyz. This is a Eulerian, grid based hydrodynamics code which is derived from gas kinetic theory. The gas density distributions and gas velocity fields resulting from these simulations were then compared to the observed galaxy morphologies and to the measured H II kinematics. The comparison enables the study of the disk dynamics as well as relative luminous-to-dark matter fractions for the sample galaxies. The inferences from this analysis, presented in detail in Chapters 4 to 6, will be now discussed in context in this final Chapter.

7.1. Results from the analysis

7.1.1. The color correction

First, a short conclusion about Bell & de Jong's color correction is given, since this correction plays a fairly important role for the project. Bell & de Jong (2001) showed, based on population synthesis models and a universal IMF, that a galaxy's color can be related to its mass-to-light ratio. This applies to a galaxy's global color as well as to local colors. Consequently, this relation can be employed to improve the estimate of the stellar surface mass density distribution, $\Sigma_\star$, of galaxies taken from the measured NIR surface brightness,

μ_K, by using color maps of the galaxy:

$$2.5 \log \Sigma_\star = -\mu_K + a_V(V-K) + c_V \qquad \text{for the example of } (V-K) \text{ color maps.} \quad (7.1)$$

Although this correction is physically motivated, its performance must be examined carefully since much of the correction relies on empirical constants a and c[1] determined from numerical studies. Bell & de Jong themselves used the relations in their paper to explore the stellar mass Tully-Fisher relation of the Ursa Major Cluster. Their results were in support of a universal stellar IMF for normal spiral galaxies.

Since this is a very recent approach that has not yet been applied in the present context, there is no reported experience with two dimensional color corrections available from the literature. Thus, it is interesting to look at the experimental evidence from this study, regarding the performance of this approach as applied to late type spiral galaxies.

At first, applying the correction maintains the radial exponential profile of spiral galaxy disks. This very basic characteristic of spiral galaxy disks can be found in optical and NIR wavelengths and reflects the overall stellar mass distribution. The color correction retains this characteristic and, moreover, it can sometimes even scale down local deviations from the pure exponential profile (e.g., for NGC 6643). Secondly, the color corrected morphology appears dynamically realistic. The correction procedure does not create features in a galaxy's disk, whose existence would require complicated dynamic processes that disagree with density wave theories or that cannot be observed in numerical experiments.

Further, the correction not only applies to population differences, but also works for moderate dust absorption ($\tau_{\rm opt} < 1$). Dust extinguishes preferentially the optical stellar light, making it dimmer. On the other hand it also reddens the stellar populations, implying a larger stellar M/L. To first order, these effects cancel out. A good example for the color correction success is again the moderately dusty NGC 6643. As expected for such a procedure, the corrected K-band radial profile appears less dust-affected than the uncorrected one (see Figure 6.19).

Despite the above cited success of the color correction for NGC 6643, the derived mass map still bears systematic uncertainties from the fact that NGC 6643 is classified as a starburst galaxy. The same applies to NGC 5676. The high luminosity end of a starburst galaxy IMF is distinctly different from the universal IMF that was adopted to derive the M/L to color relation. Bursts of star formation bias the stellar M/L to lower values at a given color. However, even for starburst galaxies the color correction provides an improved mass map as compared to the K-band. Its application is still favorable, but the bias from the starburst should be kept in mind.

Another beneficial consequence of the color correction is the fact that it accounts for the outward blueing of the disk. Color gradients are very common in disk galaxies, since the bulge is generally populated by older stars than the disk. In all the examined cases, the color correction yields a shortening of the disk scale length, which can be attributed to this effect. Interestingly, even in the K-band, which is usually considered as a quite good estimate of the stellar mass distribution, the color correction changes the radial scale length

[1] The constant c combines both empirical parameters and ones that are specific to the particular galaxy that is studied: $c = c\prime + \mu_\odot$, where $c\prime$ is the empirical constant and $\mu_\odot$ is the surface brightness of $1\,M_\odot$ at the galaxy's physical distance.

of a galaxy by about 10 %. Consequently, this causes the inferred radial force components in the disk to change their magnitude, affecting the shape of the rotation curve. However, using K-band photometry this is not a major concern when fitting rotation curves to medium resolution data because it simply implies a small change in the halo parameters (see Figure 4.2). More attention should be paid to the correction effects if the two dimensional force field within a galactic disk is studied. The non-axisymmetric forces that appear due to inhomogeneities in the stellar mass density distribution, amount to only 2 – 5 % of the total forces, however, the color correction can considerably affect them. For the galaxies in the sample, the non-axisymmetric force components changed by $\sim 30\,\%$ (median). These effects are not negligible for accurate studies.

Based on the experience gained from this project, the use of the color-correction to account for local stellar population differences is strongly encouraged when properties of galactic disks are studied which rely on their stellar mass distributions. The use of more than only two colors for the correction, could further improve the quality of the mass density distribution that can be derived.

7.1.2. Disk dynamics

The secular evolution of spiral structures in disk galaxies is an issue that has not yet been satisfyingly understood. The debate is about whether spirals arise from quasi-stationary, self-sustained density waves, or if they are transient features, triggered by internal or external processes, that fade away if not continuously replenished. However, this study is not very dependent on the long-term evolution of the spiral. The gravitational potentials used for the modelling are calculated from the morphological "snapshot" that the measurements provide and were not allowed to evolve during the simulation process. Nevertheless, one crucial assumption about the disk dynamics had to be made to link the snapshot character of the simulation to the long term evolution of the spiral pattern: It was necessary to adopt a constant pattern speed for the dominant spiral structure in time as well as in the radial extent. This is more a technical assumption that is necessary for the simulations, rather than an established result from the literature. However, in the end this approximation might not be far off. The fact that most of the simulations yield gas distributions and velocity fields that reproduce very well the observed gas properties leads to the conclusion that a quasi-stationary spiral pattern is probably a good first order approximation for all spiral galaxies from the sample. Furthermore, it must be noted that the modelling only requires that the spiral morphology is stable over about one dynamical period, the time required for the gas to adjust to moderate changes in the pattern speed. Aside from some subtle evidence that weak central bars reveal pattern rotations that are decoupled from the rest of the disk, the rigid spiral pattern assumption seems to be consistent for most of the studied disks.

7.1.2.1. Location of the corotation resonance

In light of the above, the determination of resonance locations within galactic disks actually has some meaning. With the simulation techniques described in this thesis, it is possible to measure the dynamic state of the disk from its gas kinematics. This determination is essentially independent of the density wave theory applied to explain the disk dynamics. It has been proven already that such kind of approach yields valuable information on disk

dynamics of several galaxies, like M 51 (Garcia-Burillo et al. 1993), M 100 (Garcia-Burillo et al. 1994), NGC 7479 (Sempere et al. 1995) and M 94 and NGC 3310 (Mulder & Combes 1996). However, since these studies were mostly dealing with single systems, the results were not put into a more general context.

The present study consists of a sample of five galaxies, for which it was possible to individually identify the location of the corotation resonances with a comparably high precision. Table 7.1 compiles the results for the five analyzed galaxies. Already from this rather small sample it is possible to outline general trends for spiral galaxies.

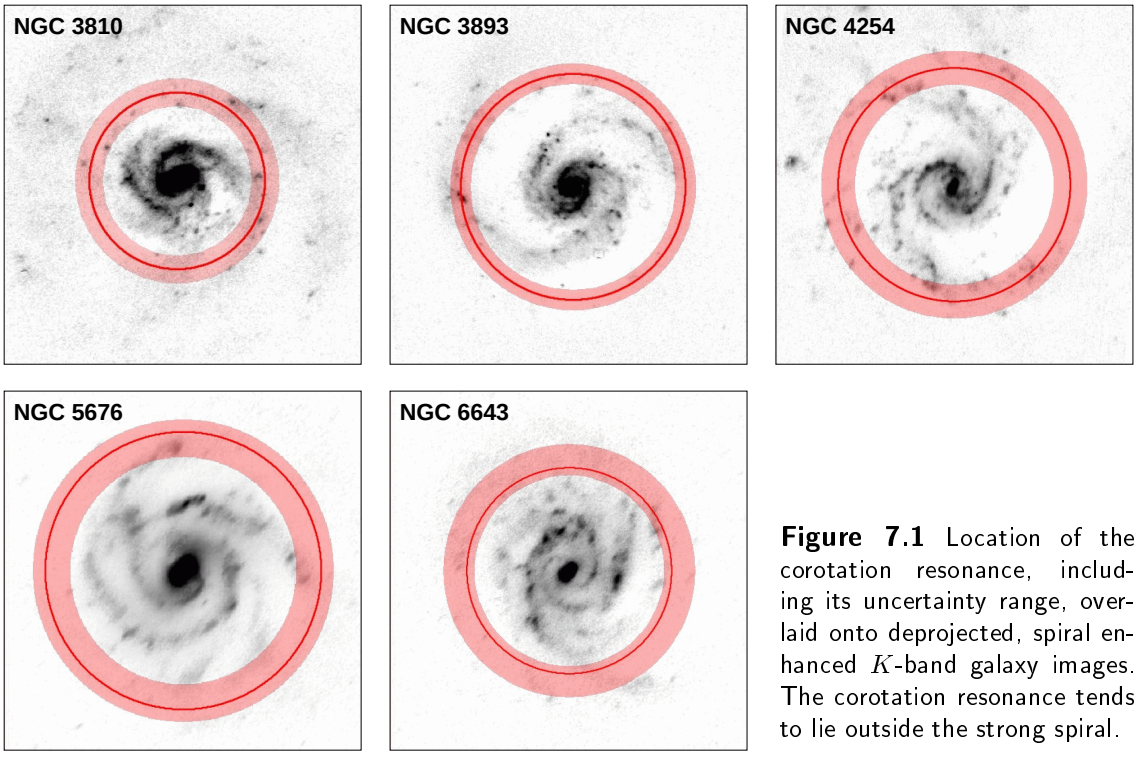

Figure 7.1 Location of the corotation resonance, including its uncertainty range, overlaid onto deprojected, spiral enhanced K-band galaxy images. The corotation resonance tends to lie outside the strong spiral.

First, one can examine the spiral morphologies and how they reflect the dynamical state of the disk. In the modal theory of spiral structure (Bertin et al. 1989a,b) the corotation resonance is typically located in the outer parts of the optical disk, where the gas-to-star density ratio is larger. The stellar spiral should exhibit a basic continuity across the corotation resonance and a reversal of the properties of the spiral tracers, such as the locations of H II-regions (Bertin 1993). As it is apparent from Figure 7.1, these predictions are only partly satisfied for the galaxies from the sample. On the other hand, some of the galaxies reveal multi-arm or flocculent spiral properties that cannot be explained by linear, quasi-stationary modal theories. Non-linear mechanisms or transient amplification processes might play important roles and affect the location of the corotation resonance too. The results from non-linear orbital modelling of spiral structures (Patsis et al. 1991) indicate that the strong, symmetric, logarithmic stellar spirals end already at the inner 4:1 resonance, located well inside the corotation resonance. In this picture, the end of the strong spiral pattern is found at a radial range of 2 – 3 exponential disk scale lengths. As seen from Figure 7.2, the corotation radii from this project's galaxy sample tend to fall in that range.

Table 7.1 Corotation radii and exponential scale lengths for the galaxies from the simulation sample, calculated for the respective distance estimation. $R_{\rm exp}(K'_{\rm corr})$ specifies the color corrected exponential scale lengths. All values are given in kpc.

Galaxy	NGC 3810	NGC 3893	NGC 4254	NGC 5676	NGC 6643
$R_{\rm CR}$	3.15 ± 0.5	5.5 ± 0.5	7.5 ± 1.1	$11.0\ ^{+1.0}_{-2.0}$	$6.5\ ^{+1.5}_{-0.5}$
$R_{\rm exp}(K')$	1.07	1.80	3.54	3.59	2.72
$R_{\rm exp}(K'_{\rm corr})$	0.913	1.74	3.06	3.12	2.48

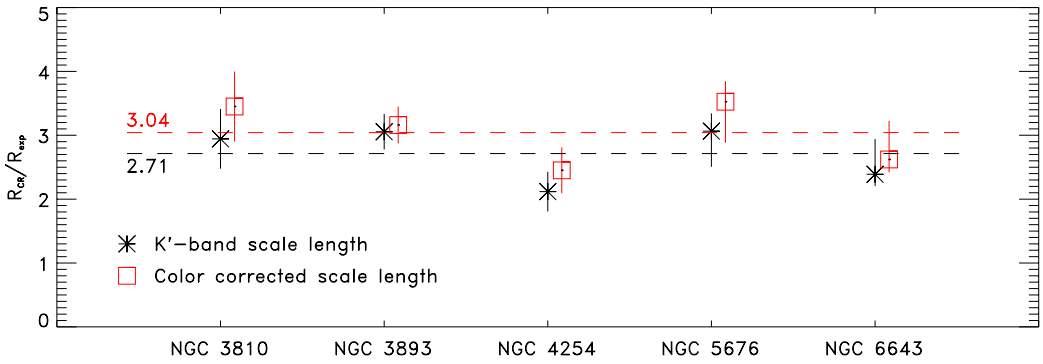

Figure 7.2 Location of the corotation radius in terms of the exponential disk scale length for the sample galaxies. The asterisks mark the values for the K-band disk, while the red boxes refer to the color corrected scale lengths. The error bars come from uncertainties in the corotation radius estimations. The horizontal lines represent the mean values.

Taking the K-band exponential disk scale length, the mean ratio of the corotation radius and the disk scale length is 2.71 ± 0.43, increasing to 3.04 ± 0.49 for the color corrected exponential disk scale lengths. Figure 7.1 compares these corotation radii to the image morphologies. Clearly, the dominant two-arm pattern in these galaxies lies mostly within the corotation resonance. This finding agrees fairly well with the conclusions of Patsis et al. (1991) and Patsis & Kaufmann (1999), derived from non-linear orbital modelling. However, also the linear modal theory of spiral structure predicts that the corotation radius falls into the radial range, which was found for the sample galaxies discussed here (Bertin 1993 states $R_{\rm CR} \approx 3-4\,R_{\rm exp}$). Thus, the locations of the corotation resonances in the sample galaxies are mostly in agreement with the predictions from linear as well as non-linear theories. The good agreement between the measured disk properties and the theoretical expectations from spiral density wave theories can be regarded in support of these theories.

Determining the location of the corotation resonance from hydrodynamic modelling is a rather elaborate and time consuming process. However, looking at Figure 7.1 it becomes clear that there is no obvious common feature in the galactic disks that would enable an easy identification of the corotation resonance otherwise. It is not always the case that at corotation the star forming rate is largely reduced. Furthermore, there is no characteristic

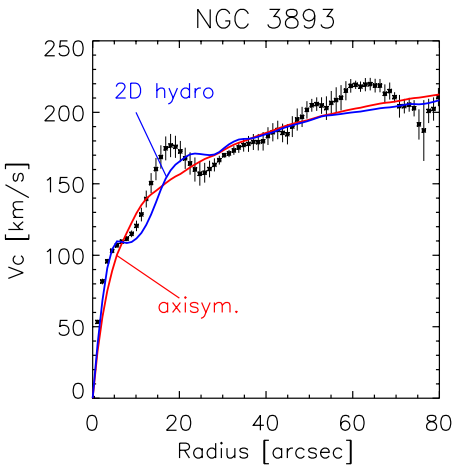

Figure 7.3 Effect of the two dimensional simulation on the average rotation curve, displayed for NGC 3893. The two dimensional fit (blue curve) provides a better general representation of the rotation curve features than the axisymmetric fit (red curve) does. However, the large wiggle is slightly misplaced.

feature in the amplitudes of the low Fourier components at the radius of the corotation resonance. This lack of any reliable corotation tracer complicates the connection between density wave theories and their application to real galaxies. Eventually, the appearance of any real galaxy in the universe is the product of a combination of many processes. In some cases, the linear modal density wave theory can be applied to describe the relevant issues, but in many galaxies non-linear effects in the density wave dynamics and other processes seem to play a role. Nevertheless, assuming a fixed spiral pattern rotation speed seems, to first order, to be a viable assumption for the simulations of gas flows in fixed galaxy potentials. In light of this, it is a very promising conclusion that the hydrodynamic gas simulations provide a powerful tool to learn about disk dynamics and to determine the location of resonances in spiral galaxies.

7.1.2.2. The disk kinematics

In addition to the good agreement of the simulated gas density distribution with the observations, the modelled gas velocity fields provide a good overall match to the measured kinematics too. In all cases, the global structure of the velocity field could be reproduced with satisfying accuracy by the model velocity field. This is a very non-trivial result which speaks highly for the fine quality of the hydrodynamics code.

Furthermore, the simulated two dimensional velocity fields also tend to render rotation curve features that can never be fitted by an axisymmetric model. This is shown for the averaged rotation curve of NGC 3893 in Figure 7.3. Although the match of the large wiggle at about $18''$ radius is not perfect, the simulated velocity field provides a better general representation of the rotation curve features.

In order to achieve the goals of this project, the above mentioned good performance of the hydrodynamic code was actually a mandatory prerequisite. The focus of the analysis was mainly on comparing the amplitude of individual wiggles and rotation curve features to the observations. To yield good results the code was required to not only reproduce global gas dynamics but also to properly model the small scale features. However, within the galactic disks, there are also other processes than local gravity fluctuations which create additional gas-dynamic effects. The gas dynamic traces of expanding supernova gas shells

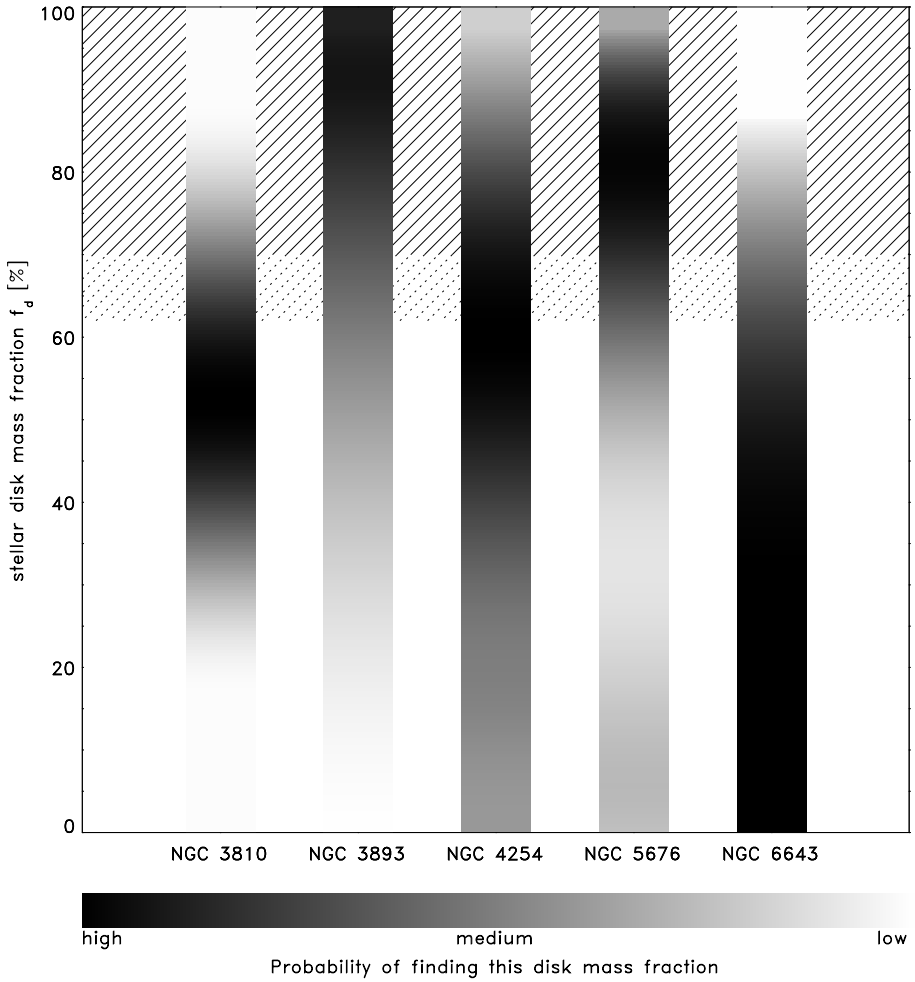

Figure 7.4 Graphical presentation of the simulation results regarding the dark matter content in the galaxies from the sample. The hashed area marks the region of maximal disks, according to the definition of Sackett (1997).

or outflows from young star forming regions are superimposed on the larger scale response to the gravitational potential wells and can eventually cover up the features that are relevant for this project. Indeed, for NGC 3810 and NGC 4254, which are galaxies with a high abundance of such "polluting" small scale velocity features in the velocity field, the model-to-data comparison allowed only less far reaching conclusions.

7.1.3. The dark matter content in the analyzed galaxies

The main objective of this study was to find the relative stellar disk to dark halo mass fractions. All conclusions were drawn from the comparison of modelled gas flows within realistic galaxy gravitational potentials of known dark and luminous matter composition. The potentials were assembled by preselecting the stellar mass contribution in terms of the maximum possible stellar mass fraction $f_d\Phi_\star$, and adding in the halo contribution to reproduce the averaged rotation curve of the galaxy. Five models were analyzed for each

galaxy with discrete values for f_d

$$\Phi_{tot}(\boldsymbol{R}|f_d) = f_d\,\Phi_\star(\boldsymbol{R}) + \Phi_{halo}(\boldsymbol{R}|f_d) \qquad \text{with } f_d = 0.2, 0.45, 0.6, 0.85 \text{ and } 1. \tag{7.2}$$

The results from the model-to-data comparison is presented in Figure 7.4 for the five galaxies NGC 3810, NGC 3893, NGC 4254, NGC 5676 and NGC 6643. The vertical axis on the five bars represent the probability that a certain mass model applies to the specific galaxy. These probabilities were determined by performing a least squares comparison between the simulated gas velocity fields and the observed kinematics of the system. As can be seen from Figure 7.4, the precision with which a certain scenario can be attributed to a particular galaxy is not equally good for all sample galaxies. For NGC 3893 the disk mass fraction could be identified very well, placing this galaxy into the realm of maximum disks. Both for NGC 3810 and NGC 6643 the least squares comparison mostly argued for a light to medium disk scenario. Especially for NGC 6643 the analysis was difficult since this galaxy exhibits only a weak stellar spiral density wave, leading to a larger uncertainty range for the disk mass fraction. The analysis of NGC 4254 suffered from the high abundance of strong non-gravitationally induced gas kinematic features in the observed velocity field. The main conclusion for NGC 4254 was to exclude the strictly maximal disk solution. For NGC 5676 the χ^2-analysis mostly argues for a heavy disk scenario, although the simulations were only partly successful, so far allowing only preliminary conclusions.

As defined by Sackett (1997), the designation "maximal disk" applies to a galactic disk when $85 \pm 10\,\%$ of the total rotational support of a galaxy at a radius $R = 2.2\ R_{exp}$ is contributed by the stellar disk mass component. In the extreme case of $v_{disk} = 0.75\,v_{tot}$, this definition allows a relatively massive halo to almost comprise the same amount of mass as the disk within that radius.

The above definition translates into the notation used here in the following way: Reading from Equation (4.12), the rotational support from the stellar disk is $v_{disk}(R_{2.2}) = \sqrt{f_d}\,v_\star(R_{2.2})$, where $v_\star(R_{2.2})$ is the rotational support from the maximal stellar disk at a radius of 2.2 disk scale lengths. Since also a maximal disk model includes a halo contribution $v_\star(R_{2.2}) = f_{max}\,v_{tot}(R_{2.2})$, with f_{max} typically 0.9. Accordingly, the rotational support from the disk is about 0.9 ($f_d = 100\,\%$), 0.83 ($f_d = 85\,\%$), 0.7 ($f_d = 60\,\%$), 0.6 ($f_d = 45\,\%$), and 0.4 ($f_d = 20\,\%$). All of the $f_d = 85\,\%$ models clearly represent maximal disk scenarios. The $f_d = 60\,\%$ models are at the lower border of the maximal disk realm, representing compositions with about an equal amount of dark and luminous mass within 2 – 3 exponential disk scale lengths.

In light of this, Figure 7.4 shows that a maximal disk scenario applies to NGC 3893 and NGC 5676. For the other galaxies the results from the modelling favor less massive stellar disks. NGC 3810, NGC 4254 and NGC 6643 possess stellar disks that appear to balance the mass of the dark halo inside the optical disk ($f_d \approx 60\,\%$), although for NGC 6643 an even lighter stellar mass component could not be excluded.

Table 7.2 gives an overview of the stellar mass-to-light ratios that could be derived from the calculations of the potentials (see Section 4.1.5). The values are given for a maximum disk and mostly fall in the range between $M/L_K = 0.6 - 0.7$. A smaller value for M/L_K was only found for NGC 4254. These stellar mass-to-light ratios agree very well with those emerging from the color correction procedure of Bell & de Jong (2001), which are

Table 7.2 Maximum disk stellar K-band mass-to-light ratios and the associated mass of the stellar disk. Given are the M/Ls, which were used to calculate the galaxy potentials and the ones that the Bell & de Jong (2001) color correction yields for the respective overall galaxy colors. The disk mass has been scaled for the galaxies' most probable disk mass fraction f_d. All values are given in solar units.

Galaxy	NGC 3810	NGC 3893	NGC 4254	NGC 5676	NGC 6643
M/L_K	0.63	0.56	0.23	0.67	0.71
M/L_{BdJ}	0.55	0.54	0.74	0.83	0.65
M_{disk}	0.89×10^{10}	2.32×10^{10}	2.12×10^{10}	8.12×10^{10}	2.54×10^{10}
f_d	60 %	100 %	60 %	85 %	60 %

based on population synthesis models[2]. Using these mass-to-light ratios, the total mass of the stellar disk can be inferred. The values given in Table 7.2 apply to a disk mass fraction which, as taken from Figure 7.4, is a reasonable assumption for the particular galaxy. These disk masses appear realistic and scale well with the maximal velocities in the rotation curves, i.e. attributing a high disk mass to NGC 5676 and a light disk to NGC 3810. The mismatch for NGC 4254 appears to be a modelling inconsistency rather than a characteristic of the galaxy. It might be related to the possibility that, after all, the disk inclination might not have been determined correctly, and that the rotation velocity and disk mass scale differently.

7.1.3.1. Discussion

Much evidence has accumulated in recent years that the disks of high surface brightness spiral galaxies dominate the dynamics of the inner regions. Most of the studies arguing for a maximal disk scenario, are based on the detailed analysis of high resolution rotation curve measurements (Blais-Ouellette et al. 1999; Palunas & Williams 2000; Ratnam & Salucci 2000; Salucci 2001). These studies, however, generally derive the rotational support of the stellar disk from an axisymmetric disk mass model and allow no consideration of non-circular rotation components. More sophisticated modelling strategies have been applied to spiral galaxies with variable significance (Erickson et al. 1999; Pignatelli et al. 2001). Mostly those studies also support heavy disks for high surface brightness galaxies but find also candidates for which lower disk mass fractions are more likely. The most convincing arguments for the maximal disk scenario come from the studies of strong bars in spiral galaxies. These features induce a strong dynamic trace in the velocity field and provide a good laboratory for estimating the stellar mass component. Based on fluid dynamic modelling, Englmaier & Gerhard (1999) find a maximal disk solution for the Milky Way and Weiner et al. (2001a) for the disk of NGC 4123. Furthermore, theoretical considerations argue for the requirement of a non-massive halo contribution in the central regions of strongly barred galaxies, because otherwise dynamical friction would slow down the bar very quickly, leading to its destruction (Debattista & Sellwood 1998, 2000).

[2]Bell & de Jong (2001) used an initial mass function that was scaled to a maximal disk scenario, which was established from measured disk kinematics. In light of this, also the population synthesis M/Ls eventually rely on disk dynamics.

However, there is also evidence that even high surface brightness spiral galaxies might be dominated by the dark matter mass component in their central disk regions. Bottema (1997) inferred from stellar velocity dispersions in spiral galaxy disks that a more massive halo component is needed to explain the findings. There are two recent studies that argue for lighter disk models by making use of previously hardly exploited, relations. Courteau & Rix (1999) applied a statistical Tully-Fisher relation analysis to a large sample of galaxies trying to relate the maximal rotation velocity of a galaxy to its disk size. Maller et al. (2000) used the geometry of a gravitational lensed system to disentangle the effects of the stellar disk and the halo mass. Both groups found that the dark halo also dynamically dominates the galaxies' inner regions.

The results from this study fit well into the overall picture that has emerged lately. Even the population of high surface brightness spiral galaxies seems to comprise not an entirely homogeneous class of objects. As it can be inferred from the maximum rotation velocity, presented in Figure 3.7, the most massive of the analyzed galaxies, NGC 3893 and NGC 5676, tend also to possess the most massive stellar disks which dominate the dynamics of the central regions. The other galaxies from the sample are less massive systems that exhibit a maximum rotation velocity $v_c < 200\,\mathrm{km\,s^{-1}}$. For those objects the total mass of the dark halo within the optical radius is higher and was found to, at least, equal the stellar mass. This trend is graphically presented in Figure 7.5. In light of this, the results from Courteau & Rix (1999) might be explained that in a statistical sample of spiral galaxies the heavy and clearly maximum disk galaxies account for only a relatively small fraction and most of the "lighter" high surface brightness galaxies exhibit already a considerable dark mass fraction.

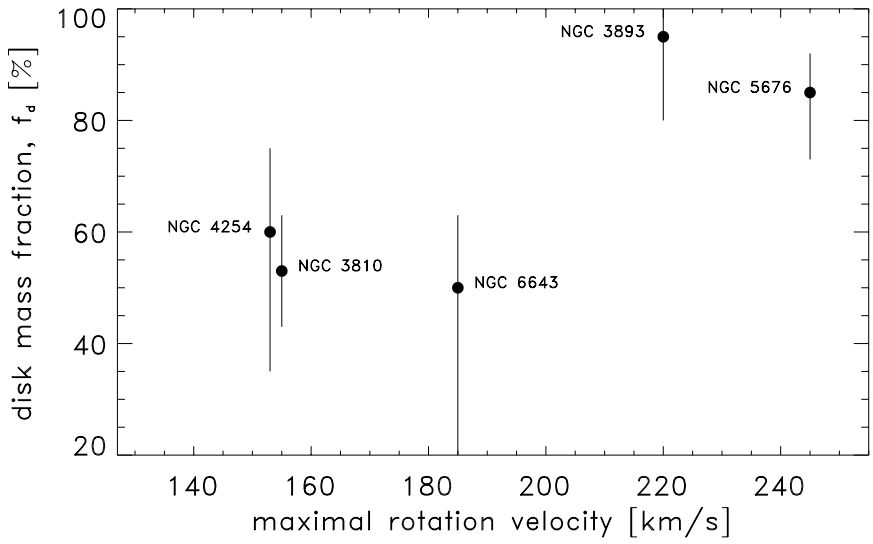

Figure 7.5 The galaxies from the analyzed sample can be separated into two classes. The most massive galaxies – as inferred from their maximum rotation velocity – tend to possess also disks with high mass fractions, f_d. Less massive systems exhibit already a considerable dark mass fraction.

However, beyond the discussion of the disk mass fraction in spiral galaxies, at present there is growing evidence that galaxy size dark halos are not cuspy in their centers, as claimed by standard cold dark matter (CDM) models. (Moore 1994, Flores & Primack 1994, Moore et al. 1999b, Salucci & Burkert 2000; Boriello & Salucci 2001; de Blok et al. 2001, van den Bosch & Swaters 2001). This circumstance was first found for low surface brightness and dwarf galaxies, that supposedly are comprised of a massive dark halo. Most of the authors argued that this also applies to high surface brightness galaxies. For the present analysis, the functional form of the dark halo profile has only a second order effect on the results as long as the models describe well the overall shape of the observed rotation curves. Thus, it was decided not to distinguish between different dark halo profiles. However, the results from this study, which mostly confirm the strong dynamic influence of the stellar disk in massive high surface brightness spiral galaxies within the optical radius, provide evidence that the halo is not particularly cuspy at its center.

After all, the dark matter research is far from presenting a conclusive and self consistent picture. The new observational evidence against standard CDM models challenge the future for the CDM cosmology and the nature of the dark matter that is involved in building our present day galaxies.

7.2. Lessons learned and outlook

It has been demonstrated with this project that an analysis similar to the one applied to barred galaxies (Englmaier & Gerhard 1999; Weiner et al. 2001) can also be applied to non-barred spiral galaxies. This fact should not be taken for granted, since the spiral arms provide a much less prominent dynamical feature in the velocity field than a strong bar does. In the end, however, the precision of the conclusion that can be drawn depends extremely on the strength of the spiral structure. If the spiral arms appear strong and well defined, significant conclusions could be drawn. A good example confirming this trend was the analysis of NGC 3893. This galaxy exhibits a clear grand design structure with strong spiral arms. The comparison of the simulations to the observations yielded a good agreement.

The reason for the strong spiral structure in NGC 3893 is the interaction with its companion NGC 3896 that triggered the density wave during a recent flyby. Due to the initial suspicion towards interacting systems for not being in a stationary state and therefore possibly presenting gas dynamics that are difficult to model, most of these systems were rejected during the sample selection. In the end, however, the contrary has turned up. As long as the galaxy is not undergoing a major merger, the interaction does not seem to spoil the analysis, but allows even wider conclusions. Apparently the gas responds rather quickly to the gravitational pull of an enhanced density wave and an equilibrium is reached rapidly. A strong gas response to a triggered density wave has also been found for other interacting systems, e.g., M81 (Visser 1980; Adler & Westpfahl 1996) and M51 (Aalto et al. 1999). Eventually, this class of objects might comprise the best suited galaxies for this kind of analysis.

Still, strong spiral arms are not the only criterion that determines the success of the analysis. NGC 4254, for example, has a very strong arm to inter-arm density contrast, but the conclusions which could be drawn were only vague. Its velocity field contains a high

abundance of small scale "noise" induced by non-gravitational gas dynamic effects (SN-bubbles, etc.). These small scale wiggles corrupt the model-to-observation comparison and complicate the identification of the best mass model. Smooth galaxy velocity fields hint for better candidates.

Considering these criteria it must be stated that the final galaxy sample, which has been made available for this study via the initial sample selection and various observing constraints, was only moderately suited. The spiral structures of NGC 3810 and NGC 6643 were very weak and posed a difficult case to enable robust conclusions from the hydrodynamic modelling. According to the experience gained from this project through the techniques described in this thesis, an ideal candidate for which one has a good chance of finding its relative dark to luminous mass fractions, exhibits strong spiral arms in NIR photometry data and a clear trace in the velocity field that is elsewhere smooth. Interactions do not necessarily spoil the success of this approach.

7.2.1. Outlook

Although this project is in principle completed, a few interesting developments are coming up in the near future that might improve the significance of results gained by such an approach. First of all, any future improvements of the code, like including gas self gravity or three dimensional capabilities, might allow an even better modelling of the gas flow. A. Slyz is continuously using the BGK hydrodynamics code for a variety of applications and its development will continue for several years.

In the same line, faster computers will allow higher grid cell numbers and therefore a better resolution of the modelled samples. Although the BGK code can also cope with low resolution grids, a better sampling of the gravitational potential will lead to a better approximation of the gas flow.

However, even if the resolution of the imaging data could not be fully applied to the modelling, high resolution data is still vitally important to create good mass maps for deriving the potentials. For nearby objects, high resolution imaging by powerful instruments (HST: WFPC2 and NICMOS, VLT: CONICA, ...) might help to get a better hold on the dust extinction effects that corrupt the quality of the observed mass maps of galaxies. On the side of the observed kinematics, sensitive high resolution integral field spectrographs (e.g., SAURON) will provide better and truly two dimensional observed gas velocity fields, that would allow a more complete comparison of the simulated gas properties to reality.

One final and very bold perspective might be to apply this strategy to probe the masses of galaxies at higher redshifts. In this way it might be possible to follow the buildup of the stellar mass in galaxies over time. However, even if this would be a very interesting project, it will not become feasible before the advent of NGST or comparable instruments.